Paramagnetic spin fluctuations in the weak itinerant-electron ferromagnet MnSi

Y. Ishikawa
Physics Department, Tohoku University, Sendai, 980, Japan

Y. Noda
Sendai Radio Technical College, Miyagi 980-31, Japan

Y. J. Uemura, C. F. Majkrzak, and G. Shirane
Brookhaven National Laboratory, Upton, New York 11973
(Received 23 October 1984)

Paramagnetic spin fluctuations in the weak itinerant-electron ferromagnet MnSi have been measured by using both unpolarized and polarized neutron scattering, and the scattering intensity was put on an absolute value by the simultaneous measurements of phonon cross sections. The magnetic excitation spectra over the whole Brillouin zone, for a wide energy range from 0 to 20 meV ($\hbar\omega/kT_c=7.9$) and up to temperatures ($T/T_c=10$) well above T_c, follow closely the Moriya-Kawabata self-consistent-renormalization theory for the weak itinerant-electron ferromagnet. Based on these experimental results, the origin of the increase in the amplitude of the local magnetic moment $\langle M_L^2 \rangle$ above T_c is attributed to the thermal excitations of the high-energy spin fluctuations in the Stoner continuum.

I. INTRODUCTION

The cubic intermetallic compound MnSi has the helimagnetic structure with a long period of 180 Å below 29.5 K.[1] It is, however, magnetically saturated in a magnetic field of 6 kOe and exhibits typical characteristics of the weak itinerant-electron ferromagnet.[2] The spontaneous magnetic moment of $0.4\mu_B$ is substantially smaller than the effective paramagnetic moment of $1.4\mu_B$ estimated from the Curie-Weiss relation of the susceptibility.[3] The previous neutron scattering measurements by Ishikawa *et al.*[4] have reported well-defined spin-wave excitations below 2.5 meV and broad excitations in the Stoner continuum at high energy. The magnetization at 10 kOe decreases with temperature much faster than that expected from the observed spin-wave excitations, suggesting that the Stoner excitations play an important role in the temperature dependence of the magnetization.[5] Additional support for this picture comes from the large magnetovolume effect below T_c.[2,5] The magnetovolume effect has the positive temperature dependence above T_c,[5] suggesting that the amplitude of the local magnetic moment on an atom $\langle M_L^2 \rangle$ increases with increasing temperature above T_c as was anticipated by Moriya's spin fluctuation theory for weak itinerant-electron ferromagnets.[6] High resolution neutron scattering measurements above T_c (Ref. 7) have demonstrated the strong temperature and wave-vector q dependence of spin fluctuations with the Lorentzian-type energy spectrum $\Gamma/(\Gamma^2+\omega^2)$ (Moriya-Kawabata fluctuations). The staggered susceptibility $\chi(q)$ obeys the relation

$$\chi(q)=\frac{C}{T-T_c+900q^2}\ , \tag{1}$$

suggesting that the Curie-Weiss law for $\chi(0)$ of MnSi is the result of these fluctuations. The linewidth Γ of the spectral distribution shows a unique q dependence,

$$\Gamma=Aq/\chi(q)=\Gamma_0 q\{[\kappa(T)]^2+q^2\}\ , \tag{2}$$

with $[\kappa(T)]^2=\kappa_0^2(T-T_c)$, in contrast with the q^2 dependence for the localized-spin system. All of these characteristics are explained by Moriya-Kawabata self-consistent-renormalization (MK SCR) theory for weak itinerant-electron ferromagnets,[8] which is later generalized in the Moriya's spin-fluctuation theory.[6]

Ishikawa also suggested in a previous paper[9] that the origin of the increase of $\langle M_L^2 \rangle$ is the result of the thermal excitations of the spin fluctuations in the Stoner continuum, the energy spectra of which has a weak temperature dependence, consistent with the spin-fluctuation theory. The argument was, however, not conclusive, because the scattering intensity was not measured on an absolute scale and therefore an accurate evaluation of the contribution of the spin fluctuations in the Stoner continuum to the susceptibility $\chi(q)$ could not be made.

A quite different model of MnSi being a heavy Fermi liquid was proposed by Ziebeck *et al.*[10] in order to explain their results of polarized neutron scattering measurements with polarization analysis. They have found that the magnetic correlation is confined to the small wave-vector region even at 580 K ($T=20T_c$) and that the paramagnetic moment $\langle M_L^2(q) \rangle$ calculated from the diffuse scattering is significantly large even below T_c ($0.84\mu_B$ at 11 K) compared with the spontaneous ferromagnetic moment of $0.4\mu_B$ and exhibits a unique temperature dependence. It increases with temperature from 11 K, taking a maximum value of $1.3\mu_B$ at 100 K, then decreases gradually with further increasing temperature. The most striking obser-

vation was the presence of a sharp peak at 0.5 Å^{-1} in the $q^2M(q)$-versus-q plot at 11 K, which they interpreted in terms of the exchange correlation hole. The peak becomes broad and is shifted to 0.6 Å^{-1} at 580 K. Since the peak was not consistent with our earlier observation,[4] Uemura *et al.*[11] performed a neutron scattering study of MnSi at 5 K by using both unpolarized and polarized neutrons and did not find any peak at 0.5 Å^{-1} in both powder and single crystal samples. Therefore, they concluded that the peak was not an intrinsic property of MnSi.

This paper is concerned with the paramagnetic spin fluctuations in MnSi and is an extension of previous work (the papers are referred to as I,[4] II,[7] and III,[9] respectively, hereafter). Recent progress[12] in the techniques for measuring the paramagnetic scattering at Brookhaven National Laboratory made it possible to determine accurately the paramagnetic scattering and to put the cross sections on an absolute scale. A systematic study of the paramagnetic state in $3d$ metals and alloys has been undertaken and the present work has been performed as a part of this program. The aim of this paper is (i) to provide the complete energy spectra of the spin fluctuations in MnSi above T_c in order to make a critical comparison with the spin-fluctuation theory and (ii) to get an insight into the paramagnetic state in the $3d$ metals in general by providing with the typical example of the paramagnetic state in an itinerant-electron system.

When this investigation started, we assumed that the MK SCR theory could apply only to a small q and ω range; we treated the cross section in the Stoner continuum as a separate entity. During the course of this investigation, the concept of paramagnetic scattering in Fe and Ni has changed dramatically.[12] The accepted picture of the propagating spin wave above T_c (Ref. 13) was challenged by a series of experiments at Brookhaven.[12] It was demonstrated[12,14] that a simple and universal paramagnetic scattering function describes the essential features of the observed paramagnetic scattering in Ni and Fe. It was suggested by Uemura *et al.*[14] that the concept of a single scattering function may apply to the high-energy excitations in MnSi as well. Our analysis of the whole magnetic cross section of MnSi in terms of the MK SCR theory has been stimulated by this suggestion.

The experimental techniques for performing the measurements as well as the method of analysis are summarized in the next section and the experimental results are presented in Sec. III, followed by discussions based on the spin-fluctuation theory.

II. EXPERIMENTAL DETAILS AND PROCEDURES FOR ANALYSIS

The crystal used in the experiment is identical to one that was employed in I and II.[4,7] The measurements were carried out on a triple-axis neutron spectrometer at the Brookhaven High Flux Beam Reactor. A pyrolytic graphite (002) monochromator and analyzer were used for unpolarized neutrons, while neutron polarization and polarization analysis were achieved by employing $Cu_2MnAl(111)$ crystals. The MnSi crystal was mounted with $(1\bar{1}0)$ vertical in a variable temperature cryostat and most of the data were taken with the constant Q mode of operation near the (110) reciprocal lattice point with the final neutron energy (E_f) being kept constant.

The paramagnetic scattering cross section $(d^2\sigma/d\omega\, d\Omega)_m$ can be separated from other scattering by employing polarized neutron beams with polarization analysis of the scattered neutrons. The following relations were used to obtain $(d^2\sigma/d\omega\, d\Omega)_m$:

$$\left[\frac{d^2\sigma^{+-}}{d\omega\, d\Omega}\right]_{\parallel} - \left[\frac{d^2\sigma^{+-}}{d\omega\, d\Omega}\right]_{\perp} = \left[\frac{d^2\sigma^{++}}{d\omega d\Omega}\right]_{\perp} - \left[\frac{d^2\sigma^{++}}{d\omega d\Omega}\right]_{\parallel} = \frac{1}{2}\left[\frac{d^2\sigma}{d\omega d\Omega}\right]_m , \tag{3}$$

where $\parallel$ and $\perp$ signs refer to the neutron scattering cross section with neutron spins parallel and perpendicular to the scattering vector, respectively. The differential magnetic cross section with one atom per unit cell is given in general by

$$\left[\frac{d^2\sigma}{d\omega\, d\Omega}\right]_m = \gamma_0^2 \frac{k_f}{k_i} |f_m(Q)|^2 2S^{\alpha\alpha}(Q,\omega) , \tag{4}$$

where

$$S^{\alpha\alpha}(Q,\omega) = \frac{\hbar}{\pi} \frac{1}{1-\exp(-\hbar\omega/kT)} \text{Im}\chi^{\alpha\alpha}(Q,\omega) \frac{1}{g^2\mu_B^2} . \tag{5}$$

This technique enabled us to determine with confidence the paramagnetic scattering at very high temperatures ($T \sim 10T_c$) even in a small energy-transfer region (MK fluctuations) where the scattering is substantially contaminated by nuclear incoherent scattering.

The absolute value of the scattering intensity $I_{\text{mag}}(Q,\omega)$ was estimated by comparing it with the integrated intensity of phonon (creation) scattering $I_{\text{ph}}(Q)$, which are given, respectively, for MnSi by

$$I_{\text{mag}}(Q,\omega) = A \frac{|F_m(Q)|^2 N}{g^2\mu_B^2 4S_i^2} 2\frac{\hbar}{\pi} \langle n+1 \rangle \text{Im}\chi^{\alpha\alpha}(Q,\omega) , \tag{6}$$

and

$$I_{\text{ph}}(Q) = AC_{\text{ph}} \frac{|F_n(Q)|^2}{\sum_i m_i} N \frac{Q^2\cos^2\theta}{\hbar\omega} \langle n+1 \rangle , \tag{7}$$

as described in detail in the Appendix.

The evaluation of the linewidth Γ of the spin-fluctuation spectra was performed by comparing the observed intensity $I^{\text{ob}}(Q,\omega)$ with the calculated intensity $I^{\text{cal}}(Q,\omega)$ which is given by

$$I^{\text{cal}}(Q,\omega) = \int \frac{d^2\sigma}{d\omega\, d\Omega}(Q',\omega') R(Q-Q',\omega-\omega') d\omega'\, dQ' , \tag{8}$$

where $R(Q-Q',\omega-\omega')$ is the resolution function of the spectrometer originally given by Cooper and Nathans and $\text{Im}\chi(Q,\omega)$ in Eq. (5) was approximated by a Lorentzian spectrum,

$$\mathrm{Im}\chi(Q,\omega)=\frac{C_{ls}}{\kappa^2+q^2}\frac{\Gamma\omega}{\Gamma^2+\omega^2}\ , \tag{9}$$

q being the momentum transfer measured from the reciprocal-lattice point.

The evaluation of the amplitude of spin fluctuations $\langle M_q^2\rangle$ from the observed spectra requires caution for an itinerant ferromagnet. By the definition, $\langle M_q^2\rangle$ can in principle be evaluated by integrating the neutron scattering function over the whole energy spectra

$$\langle M_q^2\rangle_{\mathrm{tot}}=g^2\mu_B^2\sum_\alpha\int_{-\infty}^{\infty}S^{\alpha\alpha}(Q,\omega)d\omega\ . \tag{10}$$

This is the method which Brown *et al.* have adopted[15] in their measurements; the scattered neutron's polarization was analyzed by a low energy resolution analyzer, thus achieving automatic integration of the energy of the scattered neutrons. This method, however, suffers from a serious overestimation of the $\langle M_q^2\rangle$ at low temperatures, if the energy spectra of the spin fluctuations spread over more than kT_c as is the case with MnSi. This is because the neutron energy loss scattering makes a significant contribution to the integration, even if there are no thermally excited fluctuations ($\langle n\rangle=0$), giving a larger $\langle M_q^2\rangle$ than that thermally excited. $\langle M_q^2\rangle$ by Eq. (10) includes the temperature-independent (zero-point motion) term. This will be discussed in the last section, referring to the results obtained for MnSi.

Another method is to calculate first $\chi(q)$ from the cross section by using the Krammers-Kronig relation;

$$kT\chi^{\alpha\alpha}(q)=kT\frac{1}{\pi}\int_{-\infty}^{\infty}\frac{\mathrm{Im}\chi^{\alpha\alpha}(Q,\omega)}{\omega}d\omega=kTg^2\mu_B^2\int_{-\infty}^{\infty}\frac{S^{\alpha\alpha}(Q,\omega)[1-\exp(-\hbar\omega/kT)]}{\hbar\omega}d\omega\ , \tag{11}$$

and correlate $kT\chi(q)$ with $\langle M_q^2\rangle$. This method is better than (10), because the coefficient kT excludes the zero-point motion term at low temperatures. Furthermore, $\chi(q)$ by Eq. (11) can be directly compared with the static susceptibility by extrapolating $\chi(q)$ to $q=0$. Therefore, in this paper, we adopted Eq. (11) to evaluate $\chi(q)$, and $\langle M_q^2\rangle$ was approximated[16] by $3kT\chi^{\alpha\alpha}(q)$, which is exact in the high-temperature limit ($\hbar\omega\ll kT$). However, we should note that this method possibly includes an important error for an itinerant-electron system as will be discussed in the final section. Ishikawa proposed in III (Ref. 9) another method,

$$\langle M_q^2\rangle_{\mathrm{th}}=2g^2\mu_B^2\sum_\alpha\int_{-\infty}^{0}S^{\alpha\alpha}(Q,\omega)d\omega\ , \tag{12}$$

which takes account only of the thermally excited fluctuations and omits the temperature independent term. $\langle M_q^2\rangle$ evaluated by this method would be therefore exact, if we are interested in only the temperature change. Takahashi and Moriya have also employed this method to evaluate $\langle M_q^2\rangle$ in their calculation.[17] If the fluctuation energy spectra are of order of kT, these three methods give practically the same results. In the last section we will discuss the validity of these methods based on our data for MnSi.

III. EXPERIMENTAL RESULTS

The low-energy paramagnetic scattering excitations are measured at room temperature by polarized neutron scattering with polarization analysis [Eq. (3)] as shown in Fig. 1. They were measured with $E_f=30.5$ meV and collimations of 40′-80′-80′-80′. The solid and broken lines were calculated by Eq. (8) with the value of Γ attached to each curve. The low-energy fluctuations (MK fluctuations) at 295 K clearly have the Lorentzian-type spectra for small wave vectors, but the energy spectrum is almost flat for $q=0.39$ Å^{-1} ($\zeta=0.8$), suggesting that the MK fluctuations are still confined to the small q region.

The low-energy fluctuation spectra at a momentum transfer $\zeta=\zeta_0$ and a temperature $T=T_0$ were also evaluated by unpolarized neutron scattering by subtracting the appropriate background from the observation at ζ_0 and T_0. The background was estimated from three different kinds of scattering: the scattering at $\zeta=0.6$ and 6 K, that at $\zeta=\zeta_0$ and 6 K, and that at $\zeta=0.6$ and $T=T_0$. In all of these cases the contamination by magnetic scattering has been proven to be small.[7] In Fig. 2 is shown the low-energy magnetic excitations at 270 K obtained by unpolarized neutron scattering at (0.9, 0.9, 0) and the results are compared with that obtained by polarized neutron scattering. Both data are put on an absolute scale by the procedure described in the preceding section. The solid lines are calculated by Eq. (8) with the instru-

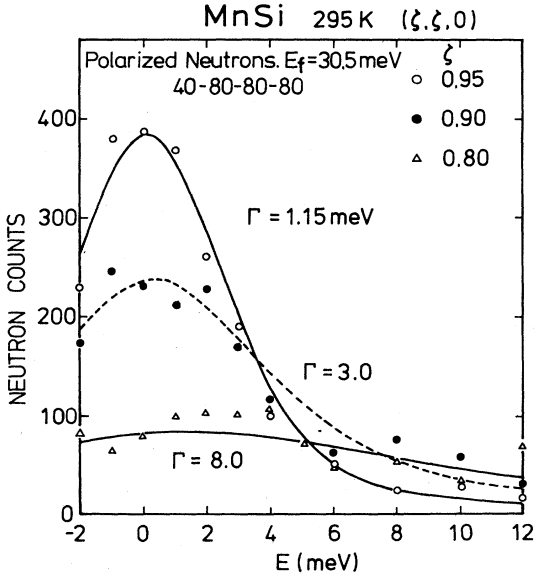

FIG. 1. Paramagnetic scattering at $(\zeta,\zeta,0)$ and 295 K measured by polarized neutrons with $E_f=30.5$ meV and with polarization analysis [see Eq. (3)]. Solid or broken lines are calculated by Eq. (8) with linewidths Γ indicated in the figure.

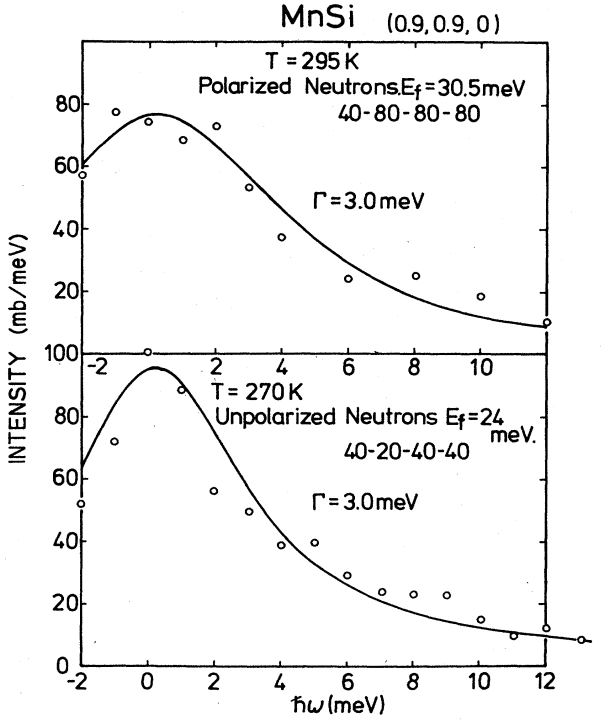

FIG. 2. Paramagnetic scattering at (0.9, 0.9, 0) measured by both polarized neutrons and unpolarized neutrons with different E_f. Absolute values were determined by the method described in the text. mb/meV in the ordinate means mb/meV sr molecule. Solid lines were calculated by Eq. (8).

mental parameters indicated in the figure. The absolute value of the calculated curve was determined so that the integrated intensity agrees with observation. The agreement between the observed unpolarized neutron scattering spectrum and the calculated contours with the linewidth $\Gamma = 3.0$ meV determined by polarized neutron scattering is quite satisfactory. This indicates that the magnetic low-energy excitations can also be estimated accurately even at 270 K by unpolarized neutron scattering. The result also provides experimental support to the validity of the present method for determining the absolute value of the paramagnetic scattering. The polarized and unpolarized neutron scattering measurements were carried out with quite different instrumental resolutions.

The paramagnetic spin fluctuations at three different temperatures of 33, 100, and 270 K were then determined by unpolarized neutron scattering over the whole magnetic Brillouin zone around (110) and up to 20 meV ($\hbar\omega = 8kT_c$). The contour maps of equal intensity for the fluctuations at these temperatures are displayed in Figs. 3(a)—3(c). The measurement could not be extended to the higher-energy side because of the presence of an optical phonon mode at about 20 meV. The contour line can be converted into the absolute scale by multiplying the value at the top of the figure [0.11 mb/meV for 3(a)] by the numbers attached to each contour line. The figure shows clearly the strong wave-vector and temperature dependences of the low-energy excitations which we called the MK fluctuations in II. The high-energy excitations, on the other hand, remain almost unchanged throughout the

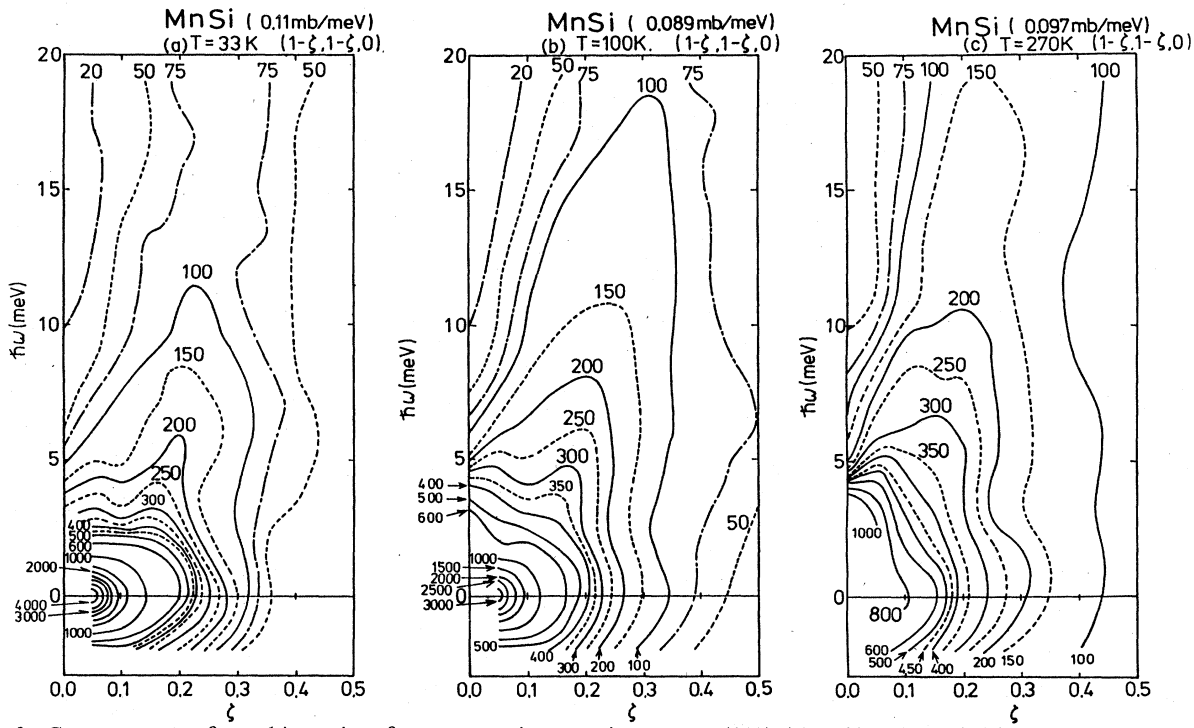

FIG. 3. Contour maps of equal intensity of paramagnetic scattering around (110), (a) at 33 K ($1.1T_c$), (b) 100 K ($3.39T_c$), (c) 270 K ($9.15T_c$), measured by unpolarized neutrons. Intensities can be put on an absolute scale by multiplying the value indicated at the top of each figure by the numbers attached to contour lines. (For example, the line with 100 is the contour of the intensity of 11 mb/meVsr molecule.) Note that the multiplication factor for the absolute value is slightly different at each temperature because of the difference in the experimental condition such as using a different cryostat, etc.

whole temperature range as was remarked in I.

The generalized susceptibility $3kT\chi(q)$ was calculated using Eq. (11) by integrating the cross section given in Fig. 3 over the energy $\hbar\omega$ after the cross section was corrected for the temperature factor $1/[1-\exp(-\hbar\omega/kT)]$ and the results are displayed in Fig. 4 as a function of the upper limit $\hbar\omega$ of the energy integration. The figure shows that at 33 K the fluctuations are mainly quasi-elastic (MK fluctuations); the curves are saturated within the energy range of instrumental resolution indicated by an arrow in the figure. There is almost no contribution to $\chi(q)$ from high-energy spectra, while at 270 K and at higher momentum transfers ($\zeta \leq 0.8$), the integration to 20 meV does not cover the whole fluctuations. The susceptibility $\chi(q)$ estimated by integration to 20 meV is plotted against wave vector $q(\zeta)$ from (1,1,0) in the [$\zeta\zeta$0] direction in Fig. 5 for three temperatures 33, 100, and 270 K [unpolarized low resolution (UPLR)]. Also plotted in the figure are the data obtained by polarized neutron scattering at 295 K [polarized low resolution (PLR), cf. Fig. 1] and those obtained by unpolarized high-resolution (UPHR) neutron scattering. The last data were taken previously[7] with the condition of $E_f = 14.8$ meV, and collimation of 20'-20'-20'-20', but the absolute intensity of scattering was newly determined by the present procedure.

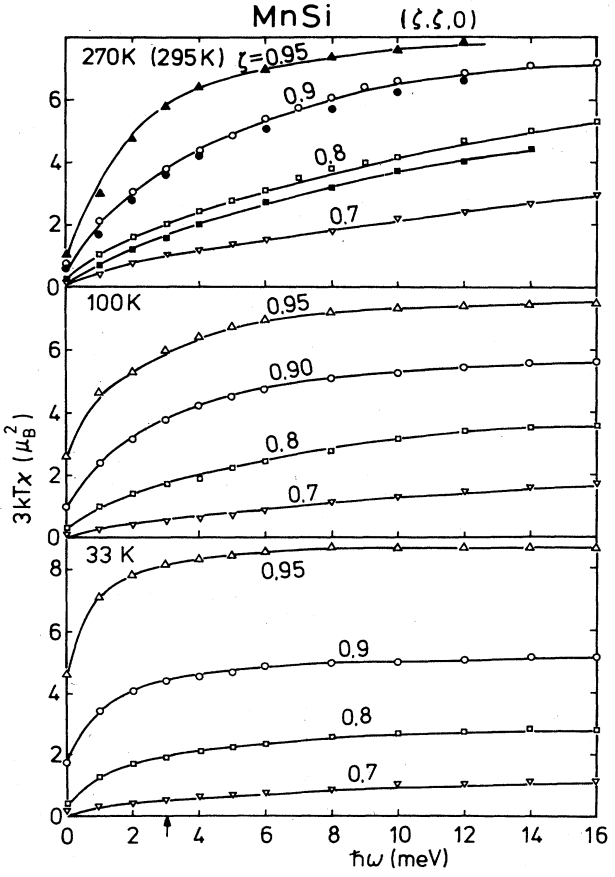

FIG. 4. Magnetic fluctuations $[3kT\chi(q)]$ obtained by integrating the scattering at $(\zeta,\zeta,0)$ in Fig. 3 up to the limiting energy on the abscissa.

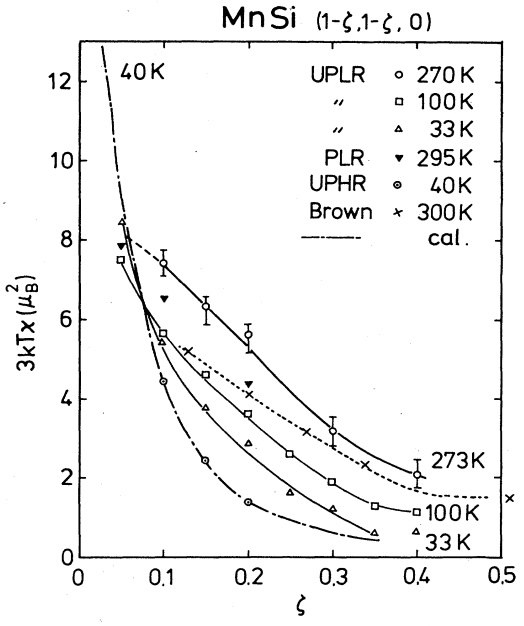

FIG. 5. Magnetic fluctuations $[3kT\chi(q)]$ by integrating the scattering at $(\zeta,\zeta,0)$ in Fig. 3 (UPLR) over $\hbar\omega$ to 20 meV plotted against ζ. The result obtained by high-resolution measurements (II) are also plotted in absolute scale. A chain line was calculated by Eq. (1), while solid and broken lines are simply guides to the eye. (UPLR, unpolarized neutron low-resolution measurement; UPHR, unpolarized neutron high-resolution measurements; PLR, polarized neutron low-resolution measurements.)

The chain line was calculated by employing Eq. (1) with $3kC = (2.1\mu_B)^2$. This relation was found to hold for the MK fluctuations between 33 and 70 K in the previous study.[7] The calculated line agrees now satisfactorily in the absolute value with the high-resolution measurement at 40 K. This provides direct experimental evidence that the MK fluctuations are the fluctuations which give the Curie-Weiss static susceptibility at $q=0$. The $\chi(q)$ evaluated from unpolarized low-resolution neutron scattering (UPLR) at 33 K is not in accord with the high-resolution measurement at 40 K on the high wave-vector side ($\zeta \leq 0.1$). This is partly due to the errors in the estimation of the high-energy fluctuations which should make a significant contribution to $\chi(q)$ by summation. This would also be the case for UPLR data at 270 K, which also deviates a little from the polarized neutron scattering data. The error bar in the data was estimated simply from the ambiguity in determining the background described in the preceding section. The result obtained by Brown *et al.*[15] by polarized neutron scattering around (000) from a powder sample agrees reasonably well with our polarized neutron data.

In order to evaluate the temperature evolution of $\langle M_L^2 \rangle$, $\sum_q \langle M_q^2 \rangle$ was approximated by $\sum_q 4\pi q^2 \times 3kT\chi(q)$ with an assumption that $\chi(q)$ is isotropic, though it is actually not the case in a strict sense.[4] $4\pi q^2 \langle M_q^2 \rangle$ at three different temperatures is plotted against $q(\zeta)$ in Fig. 6. The results exhibit a small hump at $q = 0.4$ Å^{-1} which reflects the presence of the disper-

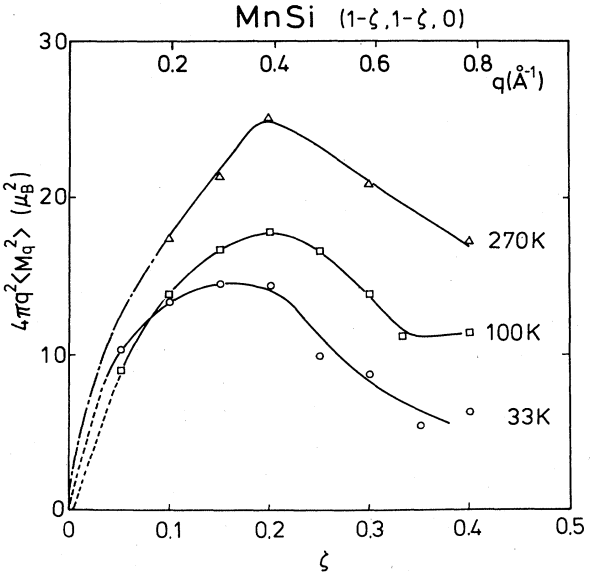

FIG. 6. $4\pi q^2\langle M_q^2\rangle$ calculated from Fig. 5 plotted against ζ. $\langle M_q^2\rangle$ was approximated by $3kT\chi(q)$.

sionlike excitation ridge in the high-energy regions [see Figs. 3(a)–3(c)]. This hump may correspond to what Ziebeck *et al.* found at 580°C.[10] The results also show clearly that $\sum_q\langle M_q^2\rangle$ increases with increasing temperature above T_c. We have shown in II that MK fluctuations below 70 K have the energy spectrum of Lorentzian shape, $\Gamma/(\Gamma^2+\omega^2)$ with $\Gamma=\Gamma_0 q(\kappa^2+q^2)$ [cf. Eq. (2)]. This relation was found to be extended to 295 K as displayed in Fig. 7 where Γ is plotted against $q(\kappa^2+q^2)$. $\kappa^2=\kappa_0^2(T/T_c-1)$ with $\kappa_0^2=0.0325$ Å^{-2}. The proportionality constant Γ_0 is 50.0 meV Å^{-3}, which is slightly different from that estimated below 70 K in II ($\Gamma_0=60.8$ meV Å^{-3}).

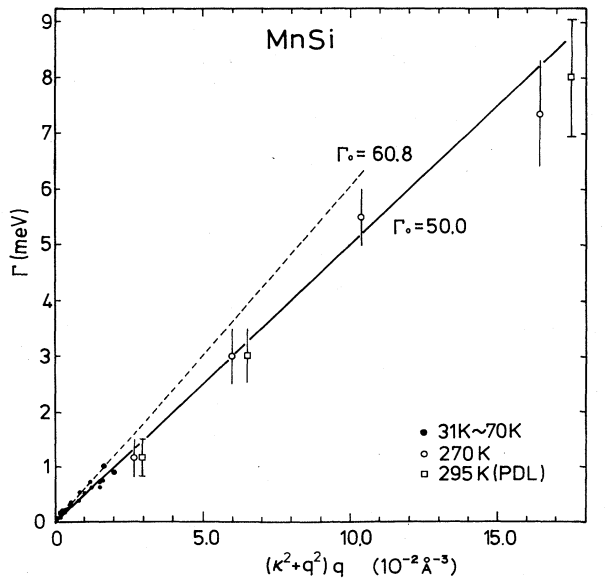

FIG. 7. Linewidth Γ obtained from low-energy excitations in Fig. 3 plotted against $(\kappa^2+q^2)q$. $\kappa^2=\kappa_0^2(T/T_c-1)$ with $\kappa_0^2=0.0325$ Å^{-2}.

IV. DISCUSSION

A. Paramagnetic scattering and spin-fluctuation theory

We have shown in II that the low-energy paramagnetic fluctuations in MnSi can be well described by the MK SCR theory.[8] The generalized susceptibility $\chi(q,\omega)$ is expressed by

$$\chi(q,\omega)=\frac{\chi_0}{1-I\chi_0(q,\omega)+\lambda(q,\omega)}\ , \tag{13}$$

where $\lambda(q,\omega)$ is a new term introduced by the MK theory[8] to go beyond the random-phase-approximation (RPA) theory and represents the mode-mode coupling.[6] In the weak itinerant-electron ferromagnetic, where only long-wave spin fluctuations are important, χ_0 can be expanded as

$$\chi_0(q,\omega)=\chi_0(0,0)[1-Aq^2+\cdots+iB(\omega/q)]\ , \tag{14}$$

and $\lambda(q,\omega)$ can be approximated by

$$\lambda(q,\omega)=\lambda(0,0)=\lambda_0 T\ . \tag{15}$$

The scattering function in Eq. (5) is then reduced to

$$S(Q,\omega)=\frac{\hbar}{\pi}\frac{1}{1-\exp(-\hbar\omega/kT)}\times\frac{C'\omega q}{\Gamma_0^2q^2[\kappa_0^2(T/T_c-1)+q^2]^2+\omega^2}\ , \tag{16}$$

with $\Gamma_0=A/B$, $\kappa_0^2=\lambda_0T_c/I_0\chi_0A$, and $C'=(1+\lambda_0T)/I\chi_0B$. This expression was also shown to be equivalent to Eq. (9) with $\Gamma=\Gamma_0q[\kappa(T)^2+q^2]$ [Eq. (2)][7] and $C_{ls}=C'$. Therefore, the scattering function has the same form as that of the localized spin system, but the constants Γ, κ, and C_{ls} have quite different characters compared with the localized spin system. The Curie-Weiss law of $\chi(0)$ is due to the linear dependence of $\lambda(0,0)$ on T.

We have shown in the preceding section that Γ obeys Eq. (2) even at 295 K. It is, therefore, of interest to examine whether Eq. (16) or Eq. (9) holds not only on the low-energy side, but also in the higher-energy region and at very high temperatures ($T\sim10T_c$). The scattering intensity was calculated by Eqs. (2), (8), and (9) with $C_{ls}/\kappa_0^2=C=(2.19\mu_B)^2$, $\kappa_0^2=0.0325$ Å^{-2}, and $\Gamma_0=50.0$ meV Å^3, and under the same instrumental conditions as those for Fig. 3. The results of calculation at 33 and 270 K are displayed in Figs. 8(a) and 8(b), which agree surprisingly well with the observation in Fig. 3. In other words, the scattering function given in Eq. (16) describes not only the low-energy part of the fluctuations—the MK fluctuations, but also higher-energy fluctuations—the excitations in the Stoner continuum. In recent studies of $3d$ ferromagnets at Brookhaven, a simple paramagnetic scattering function has been employed successfully to describe the magnetic cross section at and above T_c. Observation is, however, limited to a relatively narrow range of energy ($\hbar\omega<1.3kT_c$) and temperature ($<1.5T_c$). The situation is quite different in the present case, because

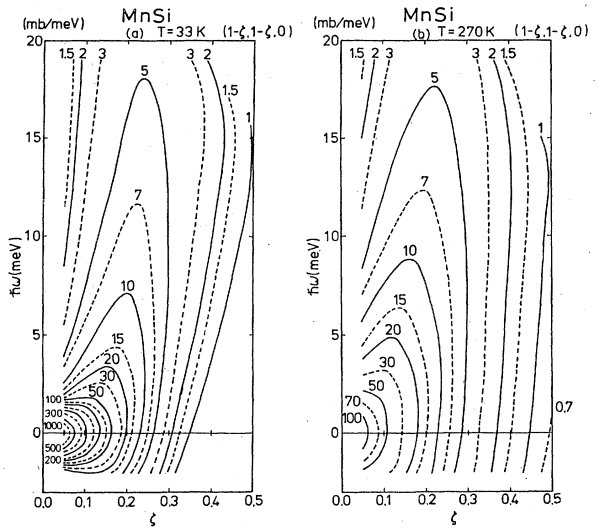

FIG. 8. Contour maps of equal intensity of paramagnetic scattering calculated by convoluting the same resolution function as in Fig. 3 with the scattering function given in Eq. (16) with $\kappa_0^2=0.0325$ Å^{-2}, $\Gamma_0=50.0$ meV Å^3, and $3kC=(2.19\mu_B)^2$; (a) 33 K and (b) at 270 K.

qualitative agreement is achieved over much wider energy and temperature regions ($\hbar\omega \lesssim 8kT_c$, $T \lesssim 10T_c$), and we therefore believe that it is truly characteristic of a weak itinerant-electron ferromagnet.

In the localized-spin system, κ_0^2 being an order of 1 [$\kappa_0^2=0.405$ Å^{-2} for EuO,[18] 1.1 Å^{-2} for Fe (Ref. 19)], the critical region where the q dependence of $\chi(q)$ is significant, is limited to a small temperature region of $T/T_c-1<0.1$ $\{[\kappa(T)]^2 \ll q^2\}$. The q dependence of $\chi(q)$ is lost when $T>5T_c$, because $\kappa(T)^2>q^2$. In MnSi, κ_0^2, being one order of magnitude smaller than that in the localized-spin system ($\kappa_0^2=0.0325$ Å^{-2}), it is natural that significant q dependence exists even at $T=10T_c$. The dependence of Γ on q is also quite substantial in MnSi. In the localized-spin system, Γ at the zone boundary is of order of kT [at $\zeta=0.5$ for Pd_2MnSn (Ref. 20)], while Γ in MnSi is about 24 meV ($9.5T_c$) at $\zeta=0.4$ and is independent of temperature. Therefore, the energy spectra at the zone boundary is almost flat with respect to $\hbar\omega$ up to 20 meV and is not modified by temperature between T_c and $10T_c$. All these characteristics are a result of the large A value in Eq. (14). Since Eq. (14) is a characteristic of the band structure of MnSi which is not modified at temperatures of order of 300 K, we can understand the remarkable results that the Lorentzian-type q and ω dependences hold over wide q, ω, and T ranges.

Another interesting problem is the origin of the sharp ridge of the high-energy spin fluctuations. We have shown in Sec. I that a ridge develops along the spin-wave dispersion at 5 K, $\hbar\omega_q=Dq^2$ with $D=52$ meV Å^2. The apparent persistent spin wave can be observed by constant E scans across the ridge.[4] Constant E scans for the cross section given in Eq. (16) exhibit a peak along the ridge ω_R,

$$\omega_R=\Gamma_0 q^3\left[1+\frac{\kappa^2}{q^2}\right]^{1/2}\left[5+\frac{\kappa^2}{q^2}\right]^{1/2}, \tag{17}$$

which becomes nearly temperature independent,

$$\omega_R \simeq \sqrt{5}\Gamma_0 q^3, \tag{18}$$

for $\zeta>0.27$, where $\kappa(T)^2/q^2<1$ even at $T=10T_c$.

This relation nearly coincides with the spin-wave dispersion in the q range of $0.2\le\zeta\le0.25$ ($0.4A^{-1}\le q\le 0.5A^{-1}$), because $\sqrt{5}q\simeq 1$ in this q range and $\Gamma_0\simeq D$. Although this argument suggests the coincidence of two relations accidental from the standpoint of RPA, there is no apparent reason why $\Gamma_0\simeq D$, since $\Gamma_0=A/B$ in Eq. (14) and D depends on the band splitting parameter. A better approximation may reveal the underlying physics for this coincidence. It has been suggested that the smooth continuation of the spin wave dispersion to the ridge of the excitations in the Stoner continuum as observed in MnSi at 5 K is a result of the many-body effect.[21] The systematic studies of other $3d$ ferromagnets[12,20] have shown the universal tendency of the constant E ridge above T_c to be near the spin-wave dispersion below T_c. This is an important subject for further studies.

The sharpness of the ridge is also related to the large Γ_0 value. The full width at half minimum Δq of the peak of the constant E scans is calculated to be

$$\frac{\Delta q}{q}\simeq\frac{\omega_R}{3\Gamma(q)}=\frac{\sqrt{5}}{3}=0.7\ . \tag{19}$$

B. Amplitude of spin fluctuations $\langle M_q^2\rangle$

For the estimate of the amplitude of the spin fluctuations $\langle M_q^2\rangle$, $3kT\chi(q)$ was calculated using Eq. (10) by summing the calculated scattering intensities for 33 and 270 K to 20 meV. The results are displayed in Fig. 9 by closed circles and triangles as a function of ζ to compare with Fig. 5. The solid lines are calculated by Eq. (1); $3kTC/[(T-T_c)+900q^2]$ with $3kC=(2.19\mu_B)^2$. The solid line by Eq. (1) at 33 K almost coincides with the calculated (Fig. 9, solid circles). This suggests that the integration over the energy to 20 meV practically includes all the fluctuations at this temperature. The slight deviation of the closed circles from the solid line are the result of a resolution effect, which is found to be not significant. The deviation of the calculated susceptibility (solid triangles) from the solid line becomes significant, however, at 270 K and for $\zeta>0.1$. This is because the integration to 20 meV is not sufficient to integrate all fluctuations.

A more important result is that the calculated values from Fig. 9 deviate substantially over the whole q range from the observed values plotted by open circles (unpolarized neutron data at 270 K) and open triangles (polarized neutron data at 295 K). The results could be interpreted to imply that the Curie-Weiss constant C is increased by 1.54 (the increase of average moment of 1.24) at 270 K compared with that at 40 K. An increase of C with temperature can be anticipated by the SCR theory as seen in Eq. (16) [$C'=(1+\lambda_0 T)/I^2\chi_0 B$]. It is noted, however, that such a large increase of the Curie-Weiss constant is

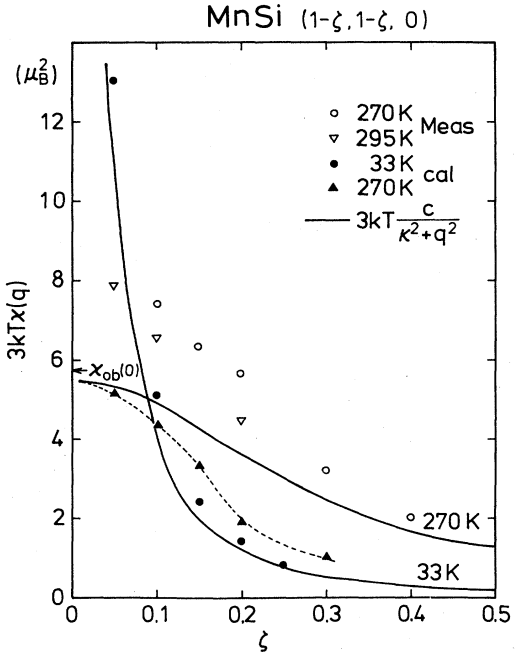

FIG. 9. Magnetic fluctuations $[3kT\chi(q)]$ calculated from Eq. (11) by integrating the scattering at $(\zeta,\zeta,0)$ in Fig. 8 over $\hbar\omega$ to 20 meV plotted against ζ(●,▲) and compared with the observed data (○,△). Solid lines are calculated by $3kTC/(\kappa^2+q^2)$ with $3kC=(2.19\mu_B)^2$ and $\kappa^2=\kappa_0^2(T-T_c)$, $\kappa_0^2=0.0325$ Å^{-2}, while a dashed line is simply a guide for the eye.

not compatible with observation. In the figure is shown by an arrow the observed value of $3kT\chi(0)$ at 270 K. The observed increase of the Curie-Weiss constant (deviation from the Curie-Weiss law) is only 6%. Therefore, the observed $\chi(q)$ is not smoothly extrapolated to $\chi(0)$. It is possible that our evaluation of the absolute value is in error by as much as 25%. Since, however, our estimated values using unpolarized and polarized neutron scattering agree with each other on the low q side, the possibility that $\chi(q)$ decreases near $q=0$ cannot be excluded. This point should be checked experimentally.

Note that the fact that the observed spin fluctuations are expressed by Eq. (9) does not mean that $\chi(q)$ of the system is given by $C_{ls}/(\kappa^2+q^2)$, because the integration of $\Gamma/(\Gamma^2+\omega^2)$ over ω cannot be extended to infinity to get $\chi(q)$. One reason is that the Lorentzian shape of the energy spectrum should be modified at the higher ω side and another is that the automatic integration to infinite energy includes the spin fluctuations not activated thermally (zero-point motion term). Therefore, it would be appropriate to perform the integration up to $\hbar\omega\simeq 2kT$. By such an integration $\chi(q)$ at 270 K does not differ significantly from that shown in Fig. 9; the q dependence of $\chi(q)$ is stronger than expected for the localized spin system even at $T=10T_c$.

Referring to Figs. 5—7, we can conclude that the origin of the increase of the amplitude of the local moment $\langle M_L^2\rangle$ above T_c in MnSi is due to the thermal activation of the high-energy component of the spin fluctuations (excitations in Stoner continuum) on the high q side ($\zeta>0.2$) as was suggested in III. This is in accord with the SCR theory. However, the increase of $\langle M_q^2\rangle$ on the low q side seems to be larger than that expected by the theory, though its contribution to $\langle M_L^2\rangle$ is not significant.

In order to evaluate the contribution of the zero-point motion to $\langle M_q^2\rangle$ at the lowest temperature, the neutron scattering intensity due to the excitations in the Stoner continuum in MnSi at 5 K given in I was put on an absolute scale by the method described in this paper and the amplitudes of the spin fluctuations $\langle M_q^2\rangle_{\rm tot}$, $\langle M_q^2\rangle_{\rm th}$, and $3kT\chi(q)$ were calculated by Eqs. (10), (11), and (12), respectively. The results are presented in Table I. The table indicates clearly that the thermally activated spin fluctuations $\langle M_q^2\rangle_{\rm th}$ or $3kT\chi$ are very small at 5 K, and the main part of the total fluctuations should therefore be attributed to the zero-point motion as suggested previously[9] and by Takahashi and Moriya.[17]

C. Linewidth Γ

We have shown that the linewidth Γ in MnSi governs the characteristics of the itinerant-electron system. In many ferromagnetic systems,[18,19,22] it has been shown that Γ obeys the scaled function

$$\Gamma=Aq^{5/2}f(\kappa/q)\ , \tag{20}$$

with a homogeneous scaling function $f(x)$ calculated by Résibois and Piette[23] for the localized-spin system. $f(x)$ tends to be 1 for $x\to 0$ (critical regime) and to $x^{1/2}$ for $x\to\infty$ (hydrodynamic regime). In order to examine the scaling hypothesis, $\Gamma/q^{5/2}$ is plotted against κ/q in Fig. 10. The figure shows that the scaling relation (20) holds within our experimental error, but $f(x)$ is quite different from the Résibois-Piette function plotted in the figure by a chain line. $f(x)$ was found to have a form $1+x^2$ shown as a broken line. The relation given by Eq. (2) gives the better scaling function as was shown in Fig. 7, though the difference is rather small.

In conclusion, the accurate determination of the spin fluctuations over the wide q and ω region up to very high temperatures has proven that MnSi exhibits the characteristics of a weak itinerant ferromagnet which can be

TABLE I. $\langle M_q^2\rangle$ in MnSi at 5 K evaluated by three different methods.

ζ	0	0.1	0.2	0.3	0.4
$\langle M_q^2\rangle_{\rm tot}(\mu_B^2)$	0.68	1.71	1.78	1.26	0.71
$\langle M_q^2\rangle_{\rm th}$	1×10^{-2}	0.8×10^{-2}	0.9×10^{-2}	0.5×10^{-2}	0.3×10^{-2}
$3kT\chi(q)$	0.6×10^{-1}	2.0×10^{-1}	2.3×10^{-1}	1.2×10^{-1}	0.5×10^{-1}

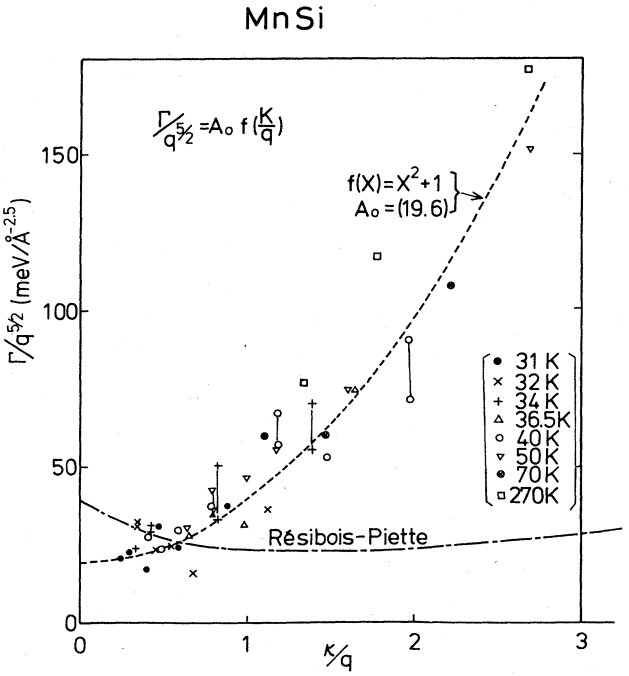

FIG. 10. Scaling of linewidth. $\Gamma/q^{5/2}$ is plotted against κ/q. A chain line is the Résibois-Piette function.

described by the SCR theory. Several objections have been raised against the idea that MnSi is a weak itinerant-electron ferromagnet. The most important claim is that the moment of $0.4\mu_B$ is relatively high for a weak itinerant-electron ferromagnet. Actually, the band calculation by Nakanishi *et al.* suggest that the intra band gap Δ is 270 meV,[24] which is significantly large compared with the observed Stoner boundary of 2.5 meV. Nakanishi, however, has also suggested[25] that the interband spin-flip transition would have a very small gap in MnSi. Therefore, the very small band gap is produced accidentally in MnSi, which plays an important definite role in making MnSi a typical weak initerant ferromagnet.

ACKNOWLEDGMENTS

This work was carried out as part of the U.S.-Japan Cooperative Neutron Scattering program. We would like to thank T. Moriya, M. Takahashi, and O. Nakanishi for helpful discussions on theoretical problems. One of the authors (Y.I.) would like to express his cordial thanks to the members of the Brookhaven Neutron Scattering Group for their kind hospitalities during his stay. Work at Brookhaven National Laboratory was supported by the Division of Material Science, U.S. Department of Energy under Contract No. DE-AC02-76CH00016.

APPENDIX: CALIBRATION OF ABSOLUTE INTENSITY USING THE PHONON INTENSITY

The observed intensity of magnetic scattering can be put onto an absolute scale by simultaneously measuring the phonon intensity.[12] For the simplest case of a system with a single atom per unit cell, the energy integrated intensity observed in constant-Q scans is given by

$$I_{\rm mag}(Q)=\tfrac{2}{3}\gamma_0^2 f_m^2(Q)S(S+1)\ , \tag{A1}$$

for paramagnetic scattering, and

$$I_{\rm ph}(Q)=C\frac{b^2}{M}\frac{Q^2\cos^2\theta}{\hbar\omega}\langle n+1\rangle\ , \tag{A2}$$

for a phonon peaking at energy $\hbar\omega$. Here $\gamma_0^2=0.291$ b, $f_m^2(q)$ is the magnetic form factor, $C=2.09$ b, b represents the scattering length, M is the atomic mass, θ denotes the angle between Q and the phonon polarization, and $\langle n+1\rangle$ gives the popularion factor. We measure the integrated intensity of a phonon, compare it to the theoretical value of Eq. (2), calibrate the instrumental efficiency, and scale the neutron intensity of magnetic scattering with this efficiency to estimate $I_{\rm mag}(Q)$ and consequently the spin S on an absolute scale.

When the magnetic intensity $I(Q,\omega)$ is measured for different energy transfers ω, we can generalize Eq. (1) by substituting $S(S+1)/3$ as

$$\tfrac{1}{3}S(S+1)\rightarrow\frac{\hbar 1}{\pi g_e^2\mu_B^2}\langle n+1\rangle{\rm Im}\chi(Q,\omega) \tag{A3}$$

to obtain the expression for the inelastic magnetic scattering intensity $I_{\rm mag}(Q,\omega)$. Indeed, $I_{\rm mag}(Q)$ of Eq. (1) represents the case when we integrate $I_{\rm mag}(Q,\omega)$ over energy ω at $kT\gg\hbar\omega$, since $S(S+1)/3$ is proportional to $kT\,{\rm Re}\chi(Q)$. In this way, we can put energy-integrated as well as inelastic magnetic scattering intensity on an absolute scale using the phonon intensity. This technique was applied to Ni (Ref. 26) and Fe (Ref. 27) to compare the experimental and theoretical intensity of magnetic scattering above T_c.

MnSi has four Mn and four Si atoms in a unit cell. Therefore, we have to extend this treatment for the case of more than one atom per unit cell. Here the scattering intensity per unit cell can be given by replacing

$$\gamma_0^2 f_m^2(Q)\rightarrow|F_m(Q)|^2/S_i^2\ , \tag{A4}$$

$$b^2/M\rightarrow|F_n(Q)|^2/\sum_i m_i \tag{A5}$$

in Eqs. (1) and (2), where $F_m(Q)$ and $F_n(Q)$, respectively, represent dynamic magnetic and nuclear structure factor, $\sum m_i$ is the mass of all the Mn and Si atoms in a unit cell, and $S_i=0.2$ is the saturation moment of the Mn atom. Then we must divide the right-hand side of Eq. (4) by four to calculate the intensity $I_{\rm mag}(Q,\omega)$ for one Mn moment

$$I_{\rm mag}(Q,\omega)=2\frac{|F_m(Q)|^2}{g^2\mu_B^2 4S_i^2}\frac{\hbar}{\pi}\langle n+1\rangle{\rm Im}\chi_{\alpha\alpha}(Q,\omega)\ . \tag{A6}$$

Since the dynamic structure factors have not been determined in MnSi, we approximate them by the static structure factors at the neighboring Bragg point. We have checked that the phonon intensities measured around different Bragg positions can be scaled reasonably well

(within the error of ±25%) by the static structure factors of each Bragg point. Since the present experiment has been carried out around the (110) Bragg point, we used the value $F_m^2 = 0.0269$ and $F_n^2 = 2.362$ b/sr. It should be noted, however, that this approximation is not accurate around the zone boundary to the (000) zone, since the static structure factors at (000) Bragg point are significantly different from that of (110).

[1]Y. Ishikawa, K. Tajima, D. Bloch, and M. Roth, Solid State Commun. **19**, 525 (1976).

[2]D. Bloch, J. Voiron, V. Jaccarino, and J. H. Wernick, Phys. Lett. **51A**, 259 (1975).

[3]H. Yasuoka, V. Jaccarino, R. C. Sherwood, and J. H. Wernick, J. Phys. Soc. Jpn. **44**, 842 (1978).

[4]Y. Ishikawa, G. Shirane, J. A. Tarvin, and M. Kohgi, Phys. Rev. **16**, 4956 (1977).

[5]M. Matsunaga, Y. Ishikawa, and T. Nakajima, J. Phys. Soc. Jpn. **51**, 1153 (1982).

[6]T. Moriya, J. Magn. Magn. Mater. 141 (1979); *Electron Correlation and Magnetism in Narrow Band Systems* edited by T. Moriya (Springer, Berlin, 1981), p. 2.

[7]Y. Ishikawa, Y. Noda, C. Fincher, and G. Shirane, Phys. Rev. B **25**, 254 (1982).

[8]T. Moriya and A. Kawabata, J. Phys. Soc. Jpn. **34**, 63 (1973); **35**, 669 (1973).

[9]Y. Ishikawa, J. Magn. Magn. Mater. **31-34**, 309 (1983).

[10]K. R. A. Ziebeck, H. Capellmann, P. J. Brown, and J. G. Booth, Z. Phys. B **48**, 241 (1982).

[11]Y. J. Uemura, C. F. Majkrzak, G. Shirane, and Y. Ishikawa, J. Appl. Phys. **55**, 1898 (1984).

[12]See, for example, a review article by G. Shirane, O. Steinsvoll, Y. J. Uemura, and J. Wicksted, J. Appl. Phys. **55**, 1887 (1984), and references therein.

[13]H. A. Mook, J. W. Lynn, and R. M. Nicklow, Phys. Rev. Lett. **30**, 556 (1973); J. W. Lynn and H. A. Mook, Phys. Rev. B **23**, 198 (1981); J. W. Lynn, *ibid.* **11**, 2624 (1975).

[14]Y. J. Uemura, G. Shirane, O. Seinsvoll, and J. Wicksted, Phys. Rev. Lett. **51**, 2322 (1983). See also Y. J. Uemura, in Proceedings of High Energy Excitations in Condensed Matter, Los Alamos National Laboratory, 1984 (in press).

[15]P. J. Brown, J. Deportes, D. Givord, and K. R. A. Ziebeck, J. Appl. Phys. **53**, 1973 (1982).

[16]Note this expression differs by a factor of 4 from that given by Brown *et al.* (Ref. 15). This is because $\chi(q)$ in their expression was defined not for moment, but for spin.

[17]Y. Takahashi and T. Moriya, J. Phys. Soc. Jpn. **52**, 4342 (1983).

[18]O. W. Dietrich, J. Als-Nielsen, and L. Passell, Phys. Rev. B **14**, 4923 (1969).

[19]M. Collins, V. Minkiewicz, R. Nathans, L. Passel, and G. Shirane, Phys. Rev. **179**, 417 (1969).

[20]G. Shirane, Y. J. Uemura, J. Wicksted, Y. Endoh, and Y. Ishikawa, Phys. Rev. B **31**, 1227 (1985).

[21]Y. Ishikawa, in *The Neutron and Its Applications* (Proceedings of Conference to mark the 50th Anniversary of the Discovery of the Neutron, Cambridge, 1982), edited by P. Schofield (IOP, London, 1983), p. 227.

[22]V. Minkiewicz, M. Collins, R. Nathans, and G. Shirane, Phys. Rev. **182**, 624 (1969).

[23]P. Résibois and C. Piette, Phys. Rev. Lett. **10**, 514 (1976).

[24]O. Nakanishi, A. Yanase, and A. Hasegawa, J. Magn. Magn. Mater. **15-18**, 879 (1980).

[25]O. Nakanishi (private communication).

[26]O. Steinsvoll, C. F. Majkrzak, G. Shirane, and J. Wicksted, Phys. Rev. Lett. **51**, 300 (1983).

[27]J. Wicksted, O. Steinsvoll, and G. Shirane, Phys. Rev. B **29**, 488 (1984).